

Preparation of Butadienylpyridines by Iridium-NHC-Catalyzed Alkyne Hydroalkenylation and Quinolizine Rearrangement

Ramón Azpíroz,^{*,[a]} Ingo Greger,^[a, b] Luis A. Oro,^[a] Vincenzo Passarelli,^[a] Ricardo Castarlenas,^{*,[a]} and Jesús J. Pérez-Torrente^{*,[a]}

Dedicated to Professor Christian Bruneau for his outstanding contribution to catalysis.

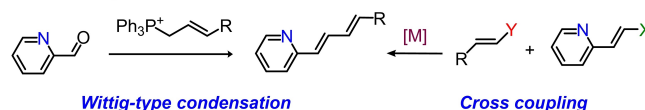
Abstract: Iridium(I) N-heterocyclic carbene complexes of formula $\text{Ir}(\kappa^2\text{O},\text{O}^-\text{BHetA})(\text{IPr})(\eta^2\text{-coe})$ [BHetA = bis-heteroatomic acidato, acetylacetonate or acetate; IPr = 1,3-bis(2,6-diisopropylphenyl)imidazolin-2-carbene; coe = cyclooctene] have been prepared by treating $\text{Ir}(\kappa^2\text{O},\text{O}^-\text{BHetA})(\eta^2\text{-coe})_2$ complexes with IPr. These complexes react with 2-vinylpyridine to afford the hydrido-iridium(III)-alkenyl cyclometalated derivatives $\text{IrH}(\kappa^2\text{O},\text{O}^-\text{BHetA})(\kappa^2\text{N},\text{C}-\text{C}_7\text{H}_6\text{N})(\text{IPr})$ through the iridium(I) intermediate $\text{Ir}(\kappa^2\text{O},\text{O}^-\text{BHetA})(\text{IPr})(\eta^2\text{-C}_7\text{H}_6\text{N})$. The cyclometalated $\text{IrH}(\kappa^2\text{O},\text{O}^-\text{acac})(\kappa^2\text{N},\text{C}-\text{C}_7\text{H}_6\text{N})(\text{IPr})$ complex efficiently catalyzes the hydroalkenylation of aromatic and aliphatic

terminal alkynes and enynes with 2-vinylpyridine to afford 2-(4*R*-butadienyl)pyridines with *Z,E* configuration as the major reaction products (yield up to 89%). In addition, unprecedented (*Z*)-2-butadienyl-5*R*-pyridine derivatives have been obtained as minor reaction products (yield up to 21%) from the elusive 1*Z*,3*gem*-butadienyl hydroalkenylation products. These compounds undergo a thermal 6π -electrocyclization to afford bicyclic 4*H*-quinolizine derivatives that, under catalytic reaction conditions, tautomerize to 6*H*-quinolizine to afford the (*Z*)-2-(butadienyl)-5*R*-pyridine by a retro-electrocyclization reaction.

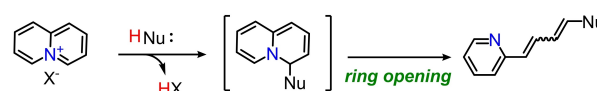
Introduction

The development of selective chemical transformations catalyzed by transition metals in C–C coupling reactions has become a powerful and versatile methodology for the preparation of high value-added organic scaffolds.^[1] In particular, π -conjugated heteroarenes, such as butadienylpyridines, are attractive synthetic goals because, beside the fact that they are valuable building blocks,^[2] they have shown interesting biological applications.^[3] Scheme 1 shows an overview of the most common routes leading to butadienylpyridines. The classical

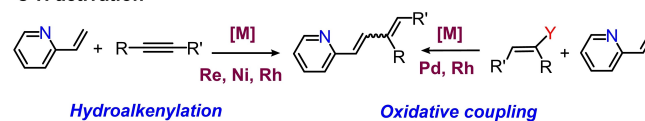
Classical synthesis



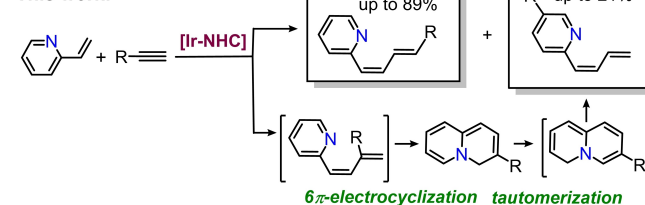
Quinolizine intermediate



C-H activation



This work:



Scheme 1. Synthetic strategies for the preparation of butadienylpyridines.

[a] Dr. R. Azpíroz, Dr. I. Greger, Prof. L. A. Oro, Dr. V. Passarelli, Dr. R. Castarlenas, Prof. J. J. Pérez-Torrente
Departamento de Química Inorgánica
Instituto de Síntesis Química y Catálisis Homogénea-ISQCH
Universidad de Zaragoza-CSIC, Facultad de Ciencias
50009 Zaragoza (Spain)
E-mail: rayazp@unizar.es
rcastar@unizar.es
perez@unizar.es

[b] Dr. I. Greger
CLARIANT, Gendorf Site
84508 Burgkirchen (Germany)

Supporting information for this article is available on the WWW under <https://doi.org/10.1002/chem.202101414>

© 2021 The Authors. Chemistry - A European Journal published by Wiley-VCH GmbH. This is an open access article under the terms of the Creative Commons Attribution Non-Commercial NoDerivs License, which permits use and distribution in any medium, provided the original work is properly cited, the use is non-commercial and no modifications or adaptations are made.

access to this type of molecules includes the Wittig-type olefination^[4] and cross-coupling reactions.^[5] However, the requirement of pre-activated substrates and the generation of

by-products are significant drawbacks. In addition, it is necessary to deal with the isomerization of the backbone double bonds since the thermodynamically favored *E,E* isomers are usually obtained.^[6] An alternative approach takes advantage of the quinolizine \rightleftharpoons butadienylpyridine tautomeric equilibrium. Even though the preparation of quinolizines is not straightforward, it has been reported that nucleophilic attack on the most common quinolizinium salts transiently generates N-bridgehead heterocycles which further evolve to the target dienyl products.^[7] More recently, also the C–H activation methodology has emerged to tackle this scenario. In this regard, a variety of palladium, nickel, rhenium or rhodium catalysts have paved the way to the functionalization of olefinic C–H protons. Specifically, this methodology has allowed to circumvent the issues arising from the dichotomous behavior of the alkenyl fragments -adding or being added- and the generally observed high dissociation energy barriers.^[8] Thus, starting from simple alkenylpyridines, oxidative couplings^[9] or total atom-economic alkyne hydroalkenylations^[10] have resulted in efficient butadienylpyridine synthesis (Scheme 1).

On another note, the advent of N-heterocyclic carbenes (NHCs) in the last two decades has represented a significant advance in organometallic catalysis^[11] and iridium chemistry has benefitted from this revolution.^[12] Indeed efficient Ir-NHC catalysts have been described for hydrogenation,^[13] hydrosilylation,^[14] H/D exchange^[15] or hydrogen borrowing strategies.^[16] However, their application in C–C coupling reactions is more limited^[17] and examples of catalytic addition of C–H across unsaturated C–C bonds are very scarce.^[18] As for the synthesis of Ir-NHC compounds, the standard preparative methods yielding complexes of general formula Ir(NHC)X(L)(L') are limited to diene, PR₃ or CO as L-type ligands. Synthesis of potentially more versatile olefin complexes (L = cyclooctene, ethylene) starting from the dinuclear precursors [Ir(μ -Cl)(η^2 -olefin)₂]₂ have been hampered by C–H activation within the wingtips of the carbene ligand.^[19]

Also relevant to this work, stoichiometric studies on the reactivity of iridium complexes have been fundamental for the understanding of mechanistic issues of C–H functionalization processes.^[20] Nonetheless, the application of iridium complexes as catalysts to this type of processes is more limited compared to rhodium. Although low-valent iridium(I) complexes are more nucleophilic than the rhodium(I) counterparts and therefore oxidative addition is more favored,^[21] the great stability of iridium(III) intermediates hampers the reductive elimination step which their rhodium analogues readily undergo.^[22] Alternatively to the C–C reductive coupling, mechanistic studies also have shown that iridium complexes can promote the C–C bond formation reactions by alkene insertion into a M–C bonds and subsequent β -hydride elimination.^[23] However, examples of alkyne hydroalkenylation are limited to functionalization of α,β -enones^[24] and intramolecular cycloisomerization of enynes.^[25]

Finally, we have recently disclosed a straightforward access to butadienylpyridines through the reaction of 2-vinylpyridine with alkynes catalyzed by Rh^I-NHC complexes.^[10c,d] However, the lack of selectivity for the *cis*-linear derivatives, due to the formation of quinolizine derivatives by thermal 6π -electrocyclic

rearrangement of branched isomers, is an important handicap. Also, the isomerization of *cis*-linear to *trans*-linear isomer was observed under catalytic conditions.

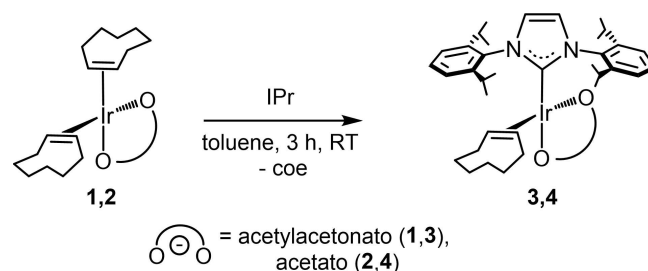
On this background we now report on the synthesis of an Ir-NHC-BHetA (BHetaA = bis-heteroatomic acidato)^[26] catalysts for the hydroalkenylation of terminal alkynes with 2-vinylpyridine yielding 2-(4*R*-butadienyl)pyridines with exclusive *Z,E* configuration along with the unprecedented 2-butadienyl-5*R*-pyridines.

Results and Discussion

Synthesis and reactivity of Ir(κ^2 O,O'-BHetaA)(IPr)(η^2 -coe) complexes

As mentioned before, it has been reported^[19] that the conversion of [Ir(μ -Cl)(L)₂]₂ into derivatives of general formula Ir(NHC)Cl(L)_n (L = cyclooctene, ethylene) is generally hampered by the C–H activation within the wingtips of the carbene ligand. Inspired by our recent results on the synthesis of rhodium(I) complexes containing the bis-heteroatomic anionic ligands (BHetaA),^[26] we envisioned that chelating ligands such as acetato (OAc) or acetylacetonato (acac) might prevent the C–H activation within the wingtips of the carbene ligand thanks to their chelating coordination mode. As a matter of fact, the iridium complexes Ir(κ^2 O,O'-BHetaA)(η^2 -coe)₂ [BHetaA = acetylacetonato (acac): **1**,^[27] acetato (OAc): **2**; coe = cyclooctene] have been revealed as useful precursors for the synthesis of mononuclear Ir(κ^2 -BHetaA)(IPr)(η^2 -coe) [IPr = 1,3-bis(2,6-diisopropylphenyl)imidazolin-2-carbene] complexes. Thus, the treatment of toluene solutions of **1** or **2** with IPr for 3 h at room temperature afforded the desired complexes Ir(κ^2 O,O'-aca-c)(IPr)(η^2 -coe) (**3**) and Ir(κ^2 O,O'-OAc)(IPr)(η^2 -coe) (**4**), which were isolated as yellow solids in yields close to 90% (Scheme 2). The clean synthesis of **3** and **4** is remarkable as the C–H activation of the isopropyl substituent of the IPr ligand is a standard outcome in this type of reactions.^[19]

The crystal structure of **3** was determined by single crystal X-ray diffraction (Figure 1). It is noteworthy that the asymmetric unit of **3** contains two crystallographically independent molecules showing very similar angles and bond lengths. Thus, only one of the two molecules is discussed herein. The crystal structure of **3** exhibits an iridium center with a slightly distorted square planar environment. The acetylacetonate acts as a bidentate ligand with a bite angle O38-Ir1-O42 of 88.32(5)°. The



Scheme 2. Preparation of Ir(κ^2 O,O'-BHetaA)(IPr)(η^2 -coe) complexes.

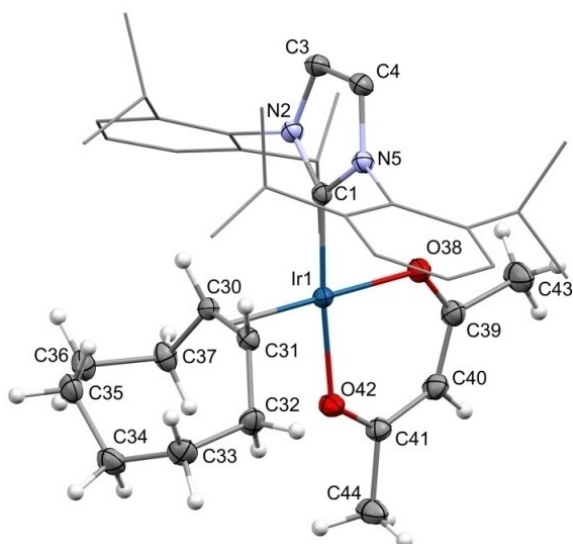


Figure 1. ORTEP plot of $\text{Ir}(\kappa^2\text{O},\text{O}'\text{-acac})(\text{IPr})(\eta^2\text{-coe})$ (**3**) with ellipsoids at 50% probability. For brevity only one of the two molecules in the asymmetric unit is shown, the other being similar (Figure S29 in the Supporting Information). Most hydrogen atoms are omitted for clarity, and a wireframe style is adopted for the 2,5-(IPr)₂C₆H₃ moiety of the IPr ligand. Selected bond lengths [Å] and angles [°] are: C1–Ir1 1.9419(17), C30–C31 1.417(2), O38–Ir1 2.0686(13), O42–Ir1 2.0706(12), Ir1–CT01 1.97648(9), O38–Ir1–O42 88.32(5), C1–Ir1–CT01 94.27(5), C1–Ir1–O38 84.67(16). CT01 is the centroid of C30 and C31.

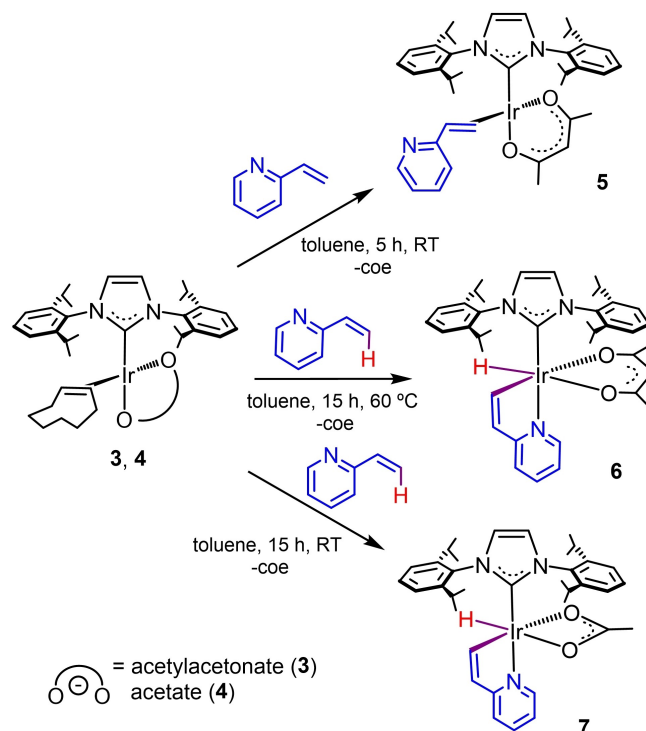
remaining coordination sites are occupied by the NHC and the coe ligands [Ir1–C1 1.9418(17) Å, Ir1–CT01 1.97548(9) Å, C30–C31 1.417(2) Å, C1–Ir1–CT01 94.27(5)°, CT01 is the centroid of C30 and C31].

As generally observed for iridium(I) olefinic complexes, the coordinated olefinic bond C30–C31 lies almost perpendicular (83.2°) to the coordination plane Ir1–C1–CT01–O38–O42. In a similar way, the NHC ring C1–N2–C3–C4–N5 adopts the least-hindered arrangement almost perpendicular (86.6°) to the above-mentioned coordination plane. Finally, as for the NHC moiety, the pitch angle θ 11.3° is indicative of a significant rotation of the NHC with respect to the N2–N5 axis, while the yaw angle ψ 0.1° indicates an almost ideal arrangement of the NHC with respect to the Ir1–C1 bond.^[28]

The ¹H and ¹³C{¹H} NMR spectra of compounds **3** and **4** in C₆D₆ confirm the presence of η^2 -cyclooctene, IPr and the corresponding acetylacetonato or acetato ligands, respectively, and are in full agreement with the solid state structure of **3**. The most noticeable feature of the ¹H NMR spectrum is the appearance of only one septuplet at around δ 3.3 ppm ($J_{\text{H+H}} \approx 6$ Hz) corresponding to the CH isopropyl protons of the IPr ligand and a shielded doublet at δ 2.9 ppm ($J_{\text{H+H}} \approx 10$ Hz) for the =CH protons of cyclooctene ligand, which is in agreement with the presence of a symmetry plane containing the O,O'-bidentate ligand and bisecting the IPr and coe ligands. However, free rotation of the IPr ligand around the Ir–C bond axis is also required to render the four CH-isopropyl protons equivalent.^[29] In addition, the ¹³C{¹H} NMR spectrum shows the characteristic resonance of the carbenic carbon atom around δ 155 ppm.^[30]

The labile character of the cyclooctene ligand in **3** and **4** allows for the exchange of that ligand with 2-vinylpyridine. However, the reaction outcome depends on both the reaction conditions and the organometallic precursor used (Scheme 3). Thus, the treatment of **3** with 2-vinylpyridine in toluene at room temperature for 5 h gave the compound $\text{Ir}(\kappa^2\text{O},\text{O}'\text{-acac})(\text{IPr})(\eta^2\text{-C}_7\text{H}_7\text{N})$ (**5**) as a result of the olefin exchange. However, reaction of **3** with 2-vinylpyridine for 15 h at 60 °C afforded the hydrido- Ir^{III} -alkenyl cyclometalated complex $\text{IrH}(\kappa^2\text{O},\text{O}'\text{-acac})(\kappa^2\text{N},\text{C-C}_7\text{H}_6\text{N})(\text{IPr})$ (**6**) which results from C–H activation of 2-vinylpyridine. In sharp contrast, the reaction of **4** with 2-vinylpyridine in toluene for 15 h at room temperature directly produced the complex $\text{IrH}(\kappa^2\text{O},\text{O}'\text{-OAc})(\kappa^2\text{N},\text{C-C}_7\text{H}_6\text{N})(\text{IPr})$ (**7**), which is analogous to **6**. It is worth noting that the putative η^2 -vinylpyridine derivative $\text{Ir}(\kappa^2\text{O},\text{O}'\text{-OAc})(\text{IPr})(\eta^2\text{-C}_7\text{H}_7\text{N})$ similar to **5** could not be detected in this case.

The crystal structure of the vinylpyridine derivatives $\text{Ir}(\kappa^2\text{O},\text{O}'\text{-acac})(\text{IPr})(\eta^2\text{-C}_7\text{H}_7\text{N})$ (**5**), $\text{IrH}(\kappa^2\text{O},\text{O}'\text{-acac})(\kappa^2\text{N},\text{C-C}_7\text{H}_6\text{N})(\text{IPr})$ (**6**), and $\text{IrH}(\kappa^2\text{O},\text{O}'\text{-OAc})(\kappa^2\text{N},\text{C-C}_7\text{H}_6\text{N})(\text{IPr})$ (**7**) were determined by single crystal X-ray diffraction. Similar to **3**, $\text{Ir}(\kappa^2\text{O},\text{O}'\text{-acac})(\text{IPr})(\eta^2\text{-C}_7\text{H}_7\text{N})$ (**5**) exhibits a distorted square planar environment for the metal center (Figure 2) featuring a bidentate acetylacetonato ligand [bite angle O30–Ir–O34 89.20(7)°], and the NHC and the vinylpyridine ligands at the remaining sites [Ir–C1 1.955(2) Å, Ir–CT01 1.98530(12) Å, C37–C38 1.418(4) Å, CT01 is the centroid of C37 and C38]. For the sake of brevity, additional structural features of **5** as well as relevant differences between the crystal structures of **3** and **5** are discussed in the Supporting Information.



Scheme 3. Reactivity of $\text{Ir}(\kappa^2\text{O},\text{O}'\text{-BHetA})(\text{IPr})(\eta^2\text{-coe})$ complexes with 2-vinylpyridine.

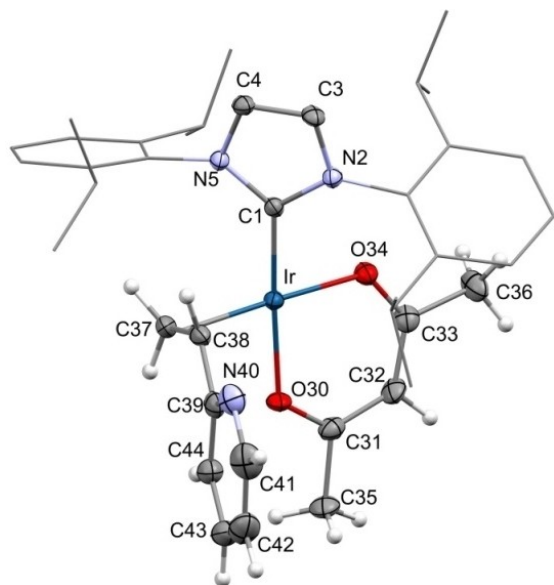


Figure 2. ORTEP plot of Ir(κ^2O,O' -acac)(IPr)(η^2 -C₇H₇N) (**5**) with ellipsoids at 50% probability. Most hydrogen atoms are omitted for clarity, and a wireframe style is adopted for the 2,6-(iPr)₂C₆H₃ moiety of the IPr ligand. Selected bond lengths [Å] and angles [°] are: Ir–C1 1.955(2), Ir–CT01 1.98530(12), Ir–O34 2.0469(17), Ir–O30 2.0644(16), C37–C38 1.418(4), O34–Ir–O30 89.20(7), C1–Ir–CT01 93.10(7). CT01 is the centroid of C37 and C38. C1–N2–C3–C4–N5: pitch angle (θ) 7.1°, yaw angle (ψ) 3.5°.

Both IrH(κ^2O,O' -acac)(κ^2N,C -C₇H₆N)(IPr) (**6**) and IrH(κ^2O,O' -OAc)(κ^2N,C -C₇H₆N)(IPr) (**7**) exhibit an octahedral environment for the metal center (Figure 3). It is worth a mention that the asymmetric unit of **7** contains two crystallographically independent molecules showing very similar angles and bond lengths. Thus, only one of the two molecules is discussed herein. In both **6** and **7** the hydrido and the NHC ligands occupy two *cis* positions [6: C1–Ir 1.990(3) Å, Ir–H 1.587(10) Å, C1–Ir–H 87.0(14)°; 7: C1–Ir1 1.983(3) Å, Ir1–H1 1.589(10) Å, C1–Ir1–H1 81.8(15)°] and the remaining coordination sites are occupied by the metallated vinylpyridine [6: C37–Ir 1.977(3) Å, N30–Ir 2.105(3) Å, C37–Ir–N30 79.21(13)°; 7: C37–Ir1 1.956(3) Å, N30–Ir1 2.084(3) Å, C37–Ir1–N30 79.12(13)°] and the acetylacetonato [6, O38–Ir 2.176(2) Å, O42–Ir 2.149(2) Å, O42–Ir–O38 86.69(9)°] or acetato moiety [7: O38–Ir1 2.283(2) Å, O40–Ir1 2.243(2) Å, O40–Ir1–O38 57.91(9)°].

In both cases, the steric hindrance of the 2,6-(iPr)₂(C₆H₃) substituents should account for the puckered conformation of the metallacycles Ir–O38–C39–C40–C41–O42 (**6**) and Ir1–O38–C39–O40 (**7**). Indeed, a puckering angle of 10.8° (**6**, between the planes Ir1–O38–O42 and O38–C39–C40–C41–O42) or 6.2° (**7**, between the planes Ir1–O38–O40 and C39–O38–O40) results in a reduced steric congestion between the 2,6-(iPr)₂(C₆H₃) substituents of the NHC ligand and the methyl group(s) of either acetylacetonate of **6** or acetate of **7**. As for the metallated vinylpyridine, the short bite angle carbon–iridium–nitrogen ($\approx 79^\circ$, see above) brings about a distorted coordination of the pyridinyl ring with yaw angles ψ of 7.4° (**6**) or 6.4° (**7**). Nonetheless, only small pitch angles of the pyridinyl moiety are observed (θ 1.6°, **6**; 1.9° **7**) reasonably as a consequence of the

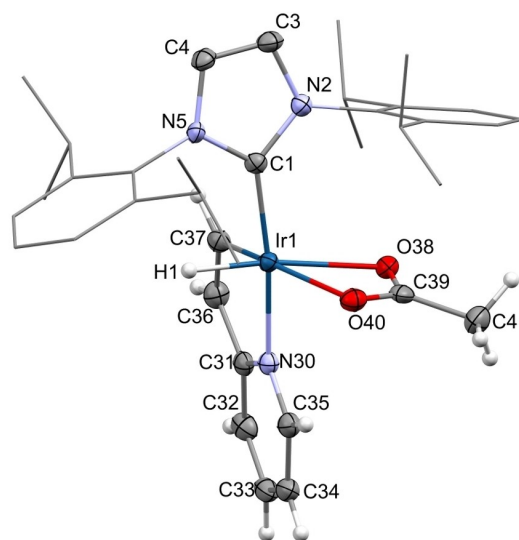
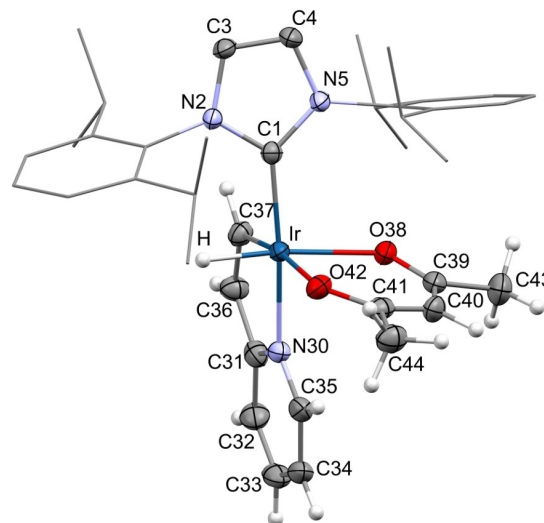


Figure 3. ORTEP view of IrH(κ^2O,O' -acac)(κ^2N,C -C₇H₆N)(IPr) (**6**, top), and IrH(κ^2O,O' -OAc)(κ^2N,C -C₇H₆N)(IPr) (**7**, bottom) with ellipsoids at 50% probability. For clarity most hydrogen atoms are omitted and wireframe style is adopted for the 2,6-(iPr)₂C₆H₃ moiety of the IPr ligand. For brevity only one of the two complexes of the asymmetric unit of **7** is shown, the other being similar (Figure S31). Selected bond lengths (Å) and angles (°) are: **6**, C1–Ir 1.990(3), C37–Ir 1.977(3), Ir–H 1.587(10), N30–Ir 2.105(3), O38–Ir 2.176(2), O42–Ir 2.149(2), C1–Ir–H 87.0(14), O42–Ir–O38 86.69(9), C37–Ir–N30 79.21(13); **7**, C1–Ir1 1.983(3), C37–Ir1 1.956(3), N30–Ir1 2.084(3), O38–Ir1 2.283(2), O40–Ir1 2.243(2), Ir1–H1 1.589(10), C1–Ir1–H1 81.8(15), O40–Ir1–O38 57.91(9), C37–Ir1–N30 79.12(13).

planarity of the bicyclic structure Ir–N30–C31–C32–C33–C34–C35–C36–C37 imposed by the sp² hybridization of its nonmetallic atoms. Also, it is noteworthy that the C36–C37 bond length in both **6** [1.353(5) Å] and **7** [1.354(5) Å] is indicative of a carbon–carbon double bond thus confirming the proposed metal–alkenyl structure. Finally, the yaw angles of the NHC moiety (ψ 1.9°, **6**; 0.2°, **7**) indicate that the NHC core minimally deviates from the ideal arrangement with respect to the iridium–carbon bond. On the other hand, similar pitch angles have been

observed (ψ 5.4°, 6; 7.6°, 7) revealing a similar rotation of the NHC moiety around the N2–N5 axis.

The NMR spectra of compounds 5–7 agree with the structure observed in the solid state. The ^1H NMR spectrum of 5 in C_6D_6 shows the expected set of shielded resonances for the η^2 -olefin moiety of the 2-vinylpyridine ligand at δ 4.24, 3.47, and 2.26 ppm ($J_{\text{H-H}} \approx 11, 8$ Hz), whereas two doublets around δ 10 and 7 ppm ($J_{\text{H-H}} \approx 8$ Hz) corresponding to the iridium-alkenyl fragment were observed for complexes 6 and 7 (Figure 4). In both cases, the proton-proton coupling constants are significantly smaller than the typical values for olefinic organic scaffolds. The ^1H NMR spectra of 6 and 7 also show a high-field shifted singlet at δ –26.70 and at –30.20 ppm,

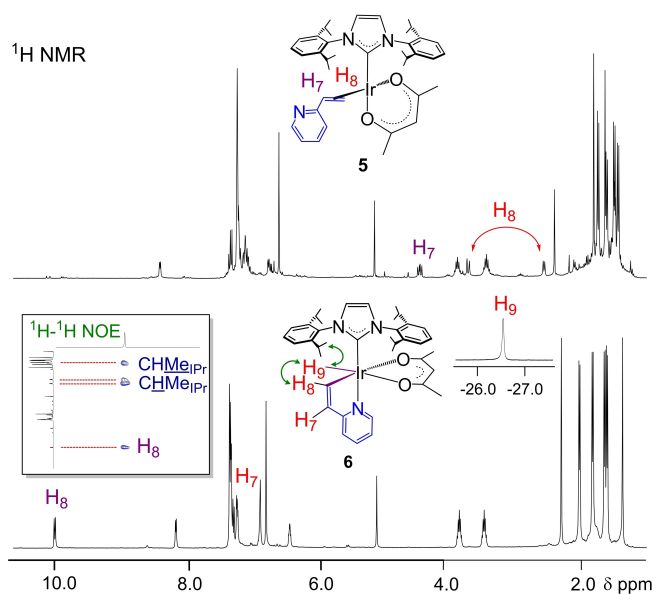
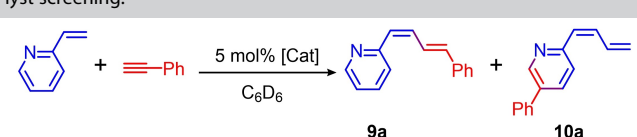


Figure 4. ^1H NMR spectra of 5 and 6 and ^1H - ^1H NOE correlations for the hydride ligand of 6.

Table 1. Hydroalkenylation of phenylacetylene with 2-vinylpyridine: catalyst screening.^[a]



Catalyst	t [h]	Conv. [%] ^[b]	Selectivity [%] ^[b]	
			9a	10a
1	1	24	12	100
2	3	24	46	84
3	5	24	53	90
4	6	2	22	86
5	6	24	95	84
6	7	2	21	90
7	7	24	55	85
8	8	1	14	21 ^[c]

[a] Reaction conditions: Catalyst (5 mol%), 0.15 mmol of 2-vinylpyridine, 0.16 mmol of phenylacetylene and 0.015 mmol of mesitylene as an internal standard in C_6D_6 (0.5 mL) at 90 °C. [b] Conversion, relative to 2-vinylpyridine, and selectivity determined by ^1H NMR. [c] Main reaction product 1,3-diphenylbut-3-en-1-yne (67%), 3-phenyl-4*H*-quinolizine (12%).

respectively, which is assigned to the hydride ligand thereby confirming the C–H activation of η^2 -olefin moiety of 2-vinylpyridine. On the other hand, the $^{13}\text{C}\{^1\text{H}\}$ NMR spectra show two singlets at δ 39.6 and 24.6 ppm which are ascribed to the coordinated alkene of 5, and a set of two singlets at around δ 160 and 128 ppm for iridium-alkenyl moiety of 6 and 7.

Hydroalkenylation of phenylacetylene: Catalyst screening

Catalytic addition of alkenyl fragments to unsaturated bonds is a powerful tool for preparation of elaborated organic structures. In view of the ability of the $\text{Ir}(\kappa^2\text{O},\text{O}^-\text{BH}et\text{A})(\text{IPr})(\eta^2\text{-coe})$ complexes to promote the C–H activation of 2-vinylpyridine to afford iridium-hydride alkenyl complexes, we decided to explore their potential as catalysts for the hydroalkenylation of alkynes with 2-vinylpyridine. Catalytic reactions were carried out in NMR tubes using 5 mol % of catalyst loading in C_6D_6 at 90 °C. A preliminary catalyst screening was performed using phenylacetylene as the model substrate (Table 1). Catalyst precursor 3 was found to be moderately active, reaching a 46% conversion of 2-vinylpyridine in 24 h and 84% selectivity for 2-((1*Z*,3*E*)-4-phenylbuta-1,3-dien-1-yl)pyridine (**9a**) resulting from *syn* addition of 2-vinylpyridine to the terminal alkyne (entry 2). The ^1H NMR spectrum of the reaction mixture showed a second set of resonances that were unequivocally ascribed to (*Z*)-2-(buta-1,3-dien-1-yl)-5-phenylpyridine (**10a**). This unexpected butadienylpyridine derivative (16%) was fully characterized by multinuclear NMR spectroscopy and selective ^1H - ^1H NOE experiments (Figure 5). A remarkable feature of the ^1H NMR spectrum of **10a** is the presence of two geminal protons at δ 5.46 and 5.42 ppm (H_{10}), each coupled with the olefinic CH proton at δ \approx 8.5 ppm (H_9), with $J_{\text{H-H}}$ of 17 and 10 Hz, respectively, thereby confirming the lack of substituents within the butadienyl fragment. Remarkably, the pyridine scaffold only contains three aromatic protons giving rise to three doublets and a ^1H - ^1H

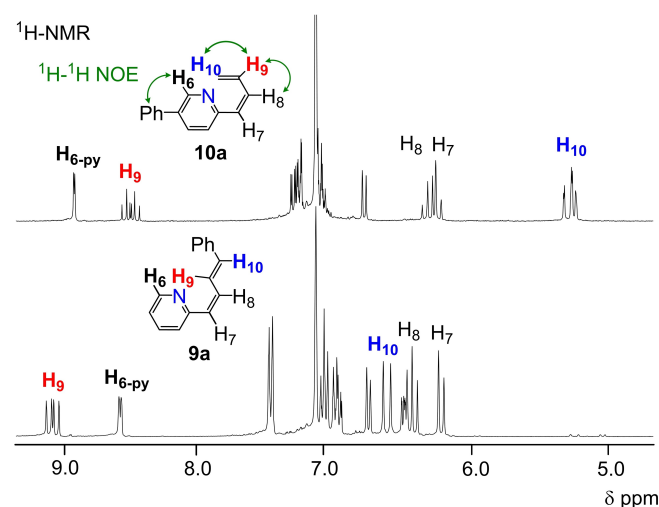


Figure 5. Selected region of the ^1H NMR spectra (CDCl_3) of 2-((1*Z*,3*E*)-4-phenylbuta-1,3-dien-1-yl)pyridine (**9a**) and (*Z*)-2-(buta-1,3-dien-1-yl)-5-phenylpyridine (**10a**) along with the proposed assignment.

NOESY correlation between the H-6 proton of the pyridine fragment and *ortho*-phenyl protons, which confirms the functionalization of the position C-3 of the pyridine (see NMR spectra in the Supporting Information). The formation of **10a** in the hydroalkenylation of phenylacetylene is indeed very striking since the phenyl ring, that should be located somewhere on the butadienyl carbon chain, ends up as a substituent in the pyridine moiety. Both butadienylpyridine derivatives **9a** (70%) and **10a** (7%) were isolated by column chromatography as colorless oils. It should be noted that the (1*Z*,3*E*)-butadienylpyridine isomer **9a** slowly isomerize to the (1*E*,3*E*) isomer at room temperature after purification. This transformation is likely promoted by light and air in the absence of catalyst at room temperature.^[4a] However, the isomerization process was not observed under catalytic conditions even at higher temperatures.

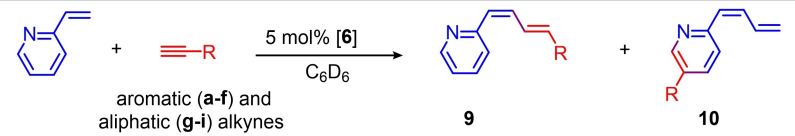
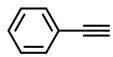
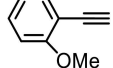
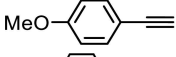
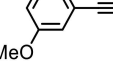

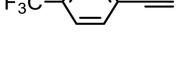
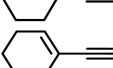
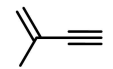
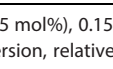
As could be expected, the catalyst precursor **5**, bearing the η^2 -2-vinylpyridine ligand, exhibited a catalytic performance comparable to that of the η^2 -cyclooctene complex **3** (entry 3). In contrast, compound **1**, which lacks the IPr ligand, was much less active affording only a 12% conversion of 2-vinylpyridine with complete selectivity to **9a** in 24 h under the same reaction conditions (entry 1). The hydrido-Ir^{III}-alkenyl cyclometalated complex **6** has turned out to be by far the most active catalyst affording a 95% conversion in 24 h with 84% selectivity for **9a**

(entry 5). Although the catalytic performance of **7** is comparable to that of **6** at short reaction times, i. e. roughly 20% of 2-vinylpyridine conversion in 2 h (entries 4 and 6), only a 55% conversion was attained after 24 h with similar selectivity for **9a** (entry 7). Finally, the rhodium catalyst precursor Rh(κ^2 O,O'-acac)(IPr)(η^2 -coe)^[31] (**8**), related to the iridium compound **3**, behaves differently affording a mixture of products including **9a** (21%), the head-to-tail alkyne dimerization product, 1,3-diphenyl-but-3-en-1-yne (67%), and 3-phenyl-4*H*-quinolizine (12%), resulting from the tautomerization of the *Z*-*gem*-butadienylpyridine hydroalkenylation product^[10c,d] (entry 8).

Hydroalkenylation of terminal alkynes: Substrate scope

Catalyst **6** was chosen for the hydroalkenylation of a range of terminal alkynes with 2-vinylpyridine using 5 mol% of catalyst loading in C₆D₆ at 90 °C (Table 2). As a general trend, aromatic terminal alkynes reacted faster than aliphatic ones and enynes (entries 1–6 vs. 7–9) to afford the 2-((1*Z*,3*E*)-4*R*-buta-1,3-dien-1-yl)pyridine (**9**) product (80–90%) and the (*Z*)-2-(buta-1,3-dien-1-yl)-5*R*-pyridine (**10**) isomer (10–20%). No relevant *Z* to *E* isomerization of the double bond in the (1*Z*,3*E*)-butadienylpyridine derivatives **9** was observed under catalytic conditions.

Table 2. Hydroalkenylation of terminal alkynes with 2-vinylpyridine catalyzed by **6**.^[a]

							
		aromatic (a-f) and aliphatic (g-i) alkynes					
Alkyne		t [h]	Conv. [%] ^[b]	Selectivity [%] ^[b]		Yield [%] ^[c]	
				9	10		
Aromatic alkynes							
1	a		24	95	84	16	70 (9a) 7 (10a)
2	b		24	92	89	11	80 (9b)
3	c		24	87	79	21	66 (9c) 13 (10c)
4	d		24	89	86	14	74 (9d)
5	e		24	87	80	20	70 (9e) 13 (10e)
6	f		72	68	88	12	54 (9f)
Aliphatic alkynes							
7	g		48	79	85	15	66 (9g)
8	h		72	84	89	11 ^[d]	62 (9h)
9	i		72	28	100	0	15 (9i)

[a] Reaction conditions: catalyst **6** (5 mol%), 0.15 mmol of 2-vinylpyridine, 0.16 mmol of phenylacetylene and 0.015 mmol of mesitylene as internal standard in C₆D₆ (0.5 mL) at 90 °C. [b] Conversion, relative to 2-vinylpyridine, and selectivity determined by ¹H NMR. [c] Isolated yield. [d] Obtained as an *E/Z* isomer mixture.

Ring-substituted phenylacetylene derivatives with electron-donating groups were efficiently transformed, albeit at slightly slower rate than phenylacetylene (entries 2–5). A slight selectivity improvement for **9b** up to 89% was observed for 1-ethynyl-2-methoxybenzene (**b**) compared to phenylacetylene (entry 2). However, up to 20% selectivity for type **10** derivatives was attained with 1-ethynyl-4-methoxybenzene (**c**) and 1-ethynyl-4-methylbenzene (**d**) (entries 3 and 5). In contrast, a sharp activity decrease was observed for electron-withdrawing substituent on the phenyl ring, such as the $-\text{CF}_3$ group, with a conversion of 2-vinylpyridine of 68% in 72 h, and a slight selectivity improvement for **9f** compared to phenylacetylene (entry 6). An activity decrease was also observed in the hydroalkenylation of aliphatic terminal alkynes such as 1-hexyne (**g**) and 1-ethynylcyclohex-1-ene (**h**). Conversions higher than 80% were attained in 48 and 78 h, respectively, with good selectivity for the corresponding (*Z,E*)-butadienyl products **9g** and **9h**, without observable isomerization (entries 7 and 8). In contrast to **10g**, which was selectively obtained as the *Z* isomer, compound **10h** was obtained as an *E/Z* isomer mixture. On the other hand, the hydroalkenylation of 2-methylbut-1-en-3-yne (**i**) selectively afforded **9i** although at low conversion level (entry 9). The butadienylpyridine derivatives **9a–9h**, **10a**, **10c** and **10e** were isolated by column chromatography as colorless oils (Table 2).

Mechanistic studies

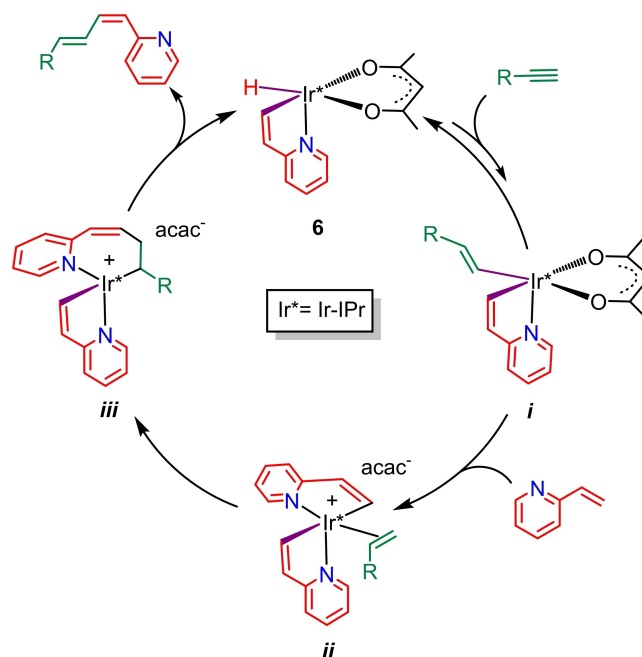
A straightforward mechanism for the formation of butadienylpyridines by the iridium-alkenyl-hydride catalyst **6** could involve the coordination of the alkyne, 1,2-insertion into the Ir–H bond and reductive elimination of the two alkenyl fragments. In order to validate this hypothesis, we have studied the reactivity of **6** with phenylacetylene. Thus, an NMR tube was charged with a solution of **6** in C_6D_6 and 3 equiv. of phenylacetylene (**a**). No reaction was observed at either RT or 60 °C for 1 h. Further heating for 24 h at 60 °C resulted in catalyst decomposition without formation of any butadienylpyridine product. However, heating a solution of **6** in C_6D_6 containing phenylacetylene (3 equiv) and 2-vinylpyridine (3 equiv) at 60 °C for 1 h resulted in the formation of the butadienylpyridine product **9a**. These observations suggest that the reaction mechanism is more complex than initially thought. Relevant to the following mechanistic proposal, a related precedent in the Ir–P/Pr₃ chemistry was previously reported by one of us.^[23] In particular, it has been shown that reductive elimination in the bis-alkenyl $[\text{Ir}(\text{alkenyl})(\kappa^2\text{N,C-C}_7\text{H}_6\text{N})(\text{NCCH}_3)_2(\text{P}i\text{Pr}_3)]^+$ complex does not take place under thermal conditions. However, stoichiometric reactivity studies showed that 2-vinylpyridine cleanly promoted the C–C coupling reaction through a η^2 -alkene intermediate complex.^[23]

On this background, the proposed mechanism for the hydroalkenylation of terminal alkynes with 2-vinylpyridine catalyzed by **6** entails the coordination of the alkyne, facilitated by the κ^1 coordination of the acac ligand, which is followed by insertion into the Ir–H bond, likely with 1,2-regioselectivity due to the steric hindrance exerted by the bulky NHC ligand, to

afford a bis-alkenyl intermediate (*i*). This species might react with 2-vinylpyridine to afford a cationic species featuring two $\kappa^2\text{N,C}$ -alkenyl-pyridine ligands and the η^2 -coordinated alkene R-CH=CH_2 , (*ii*). The formation of this intermediate should proceed from the C–H activation of 2-vinylpyridine by a σ -CAM mechanism (σ -complex-assisted metathesis)^[32] or, alternatively, via a two-step reaction via an Ir^v species. Subsequent alkene insertion into the coplanar iridium-alkenyl bond may afford an unsaturated Ir^{III} intermediate (*iii*), featuring a seven-membered ring resulting from the C–C coupling reaction, from which β -hydride elimination leads to the formation of (1*Z*,3*E*)-butadienylpyridines (**9**) with regeneration of the hydrido-iridium catalytic active species **6** (Scheme 4).

An alternative mechanism involving the initial reaction of **6** with 2-vinylpyridine has been also considered. In that case, the release of the (1*Z*,3*E*)-butadienylpyridine product in the final step would afford the iridium(I) species $\text{Ir}(\kappa^2\text{-O,O'acac})(\text{IPr})(\eta^2\text{-C}_7\text{H}_7\text{N})$ (**5**) that was established (see above) to be less active than **6**, thus that mechanism should be discarded (see the Supporting Information).

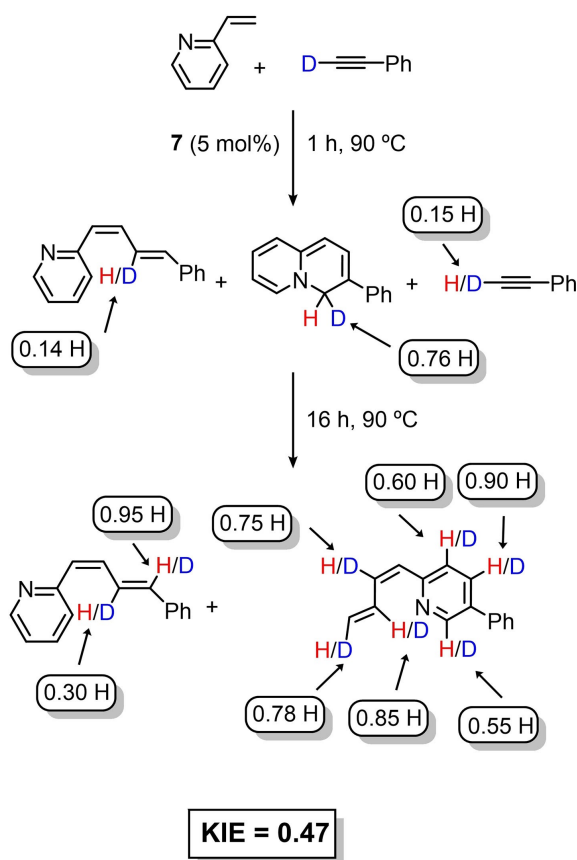
The mechanism depicted in Scheme 4 is consistent with the observation of traces of terminal alkenes at the end of the catalytic tests (¹H NMR). A ¹H NMR kinetic study comparing the reaction rate for the hydroalkenylation of phenylacetylene and [D]phenylacetylene gave a Kinetic Isotopic Effect (KIE) of 0.47 ± 0.05 (see the Supporting Information). This value suggests that the C–H cleavage does not occur in the rate-determining step, however denotes the presence of an important inverse secondary isotope effect.^[33] In general terms, inverse kinetic isotope effect has been attributed to an inverse equilibrium isotope effect (EIE)^[34] or to the formation of alkane σ -complex intermediates.^[35] In this regard, the presence of the anionic acac



Scheme 4. Proposed mechanism for the hydroalkenylation of alkynes with 2-vinylpyridine leading to **9**.

ligand could assist the stabilization of catalytic intermediates through a CH...acac interaction thus hampering the insertion processes in the step $i \rightarrow ii$. In addition, assuming the alkene insertion into the iridium-alkenyl bond as the rate-determining step ($ii \rightarrow iii$), the occurrence of a transition state with sp^3 character due to a change of hybridization from sp^2 to sp^3 could also account for the observed inverse kinetic isotope effect.^[34]

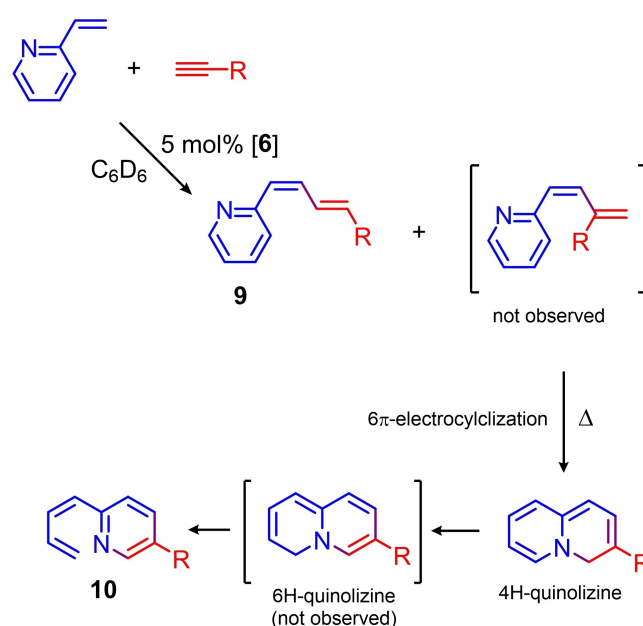
In order to gain insight into the reaction mechanism, a deuterium labeling experiment involving [D]phenylacetylene has been performed (Scheme 5). Thus, the treatment of 2-vinylpyridine with [D]phenylacetylene (0.15 mmol) in C_6D_6 (0.5 mL) in the presence of **6** (5 mol%) resulted in the formation of both hydroalkenylation products **9a** and **10a** after 16 h at 90 °C (Scheme 5). Exclusive deuteration of the *E*-olefin moiety of the butadienyl fragment was observed for **9a**, which is in accordance with our mechanistic proposal depicted in Scheme 4 and discards the vinylpyridine insertion into the Ir–H bond. In addition, deuterium incorporation was found at practically all positions of pyridine and butadienyl fragments of **10a** indicating a tautomerization process in the pyridine ring (see below). The detection of the N-bridgehead heterocyclic compound 4*H*-quinolizine in the reaction of 2-vinylpyridine with [D]phenylacetylene at the beginning of the reaction (1 h) has provided a key clue to understand the formation of the unexpected butadienylpyridine derivative **10a**.



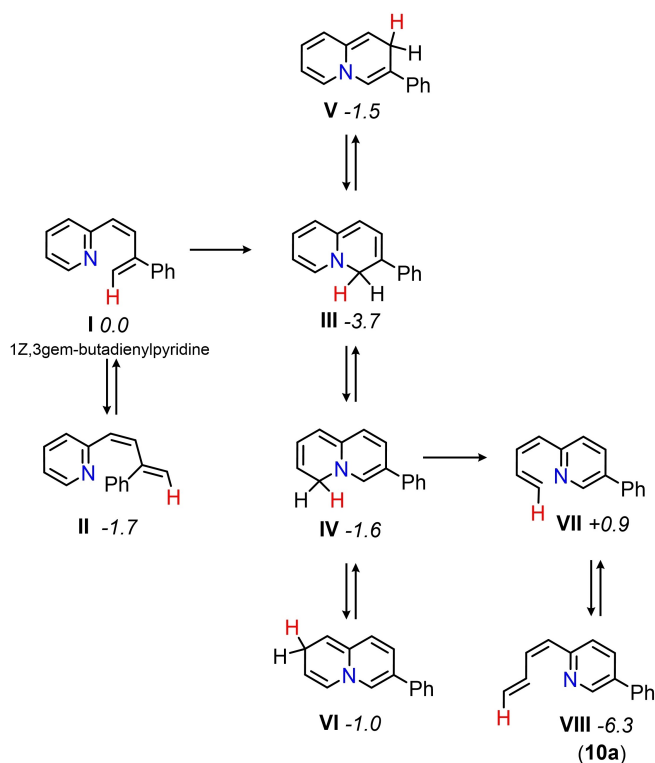
Scheme 5. Deuterium-labeling experiment: hydroalkenylation of [D] phenylacetylene with 2-vinylpyridine catalyzed by **6**.

In this regard, we have recently described the outstanding catalytic performance of Rh-NHC catalysts in C–C coupling reactions leading to the formation of 4*H*-quinolizine derivatives under mild reaction conditions.^[10c,d] These bicyclic compounds result from the thermal 6π -electrocyclization of 1*Z*,3*gem*-butadienylpyridine derivatives formed in the hydroalkenylation reactions. Thus, we might hypothesize that the alkyne hydroalkenylation reactions catalyzed by **6** result in the formation of the butadienyl products 2-((1*Z*,3*E*)-4*R*-buta-1,3-dien-1-yl)pyridine (**9**) and the putative 2-((1*Z*,3*gem*)-3*R*-buta-1,3-dien-1-yl)pyridine roughly in a 4:1 ratio (Scheme 6). The latter compound might undergo a thermal 6π -electrocyclization involving the two conjugated double bonds and one C=N of the pyridine moiety to afford the 4*H*-quinolizine skeleton. At this point, basic or acid mediated tautomerization to 6*H*-quinolizine could take place, followed by C–N bond cleavage to straightforwardly afford the (*Z*)-2-(buta-1,3-dien-1-yl)-5*R*-pyridine (**10**) derivatives (Scheme 6).

It is worth noting that the undetected 2-((1*Z*,3*gem*)-3*R*-buta-1,3-dien-1-yl)pyridine intermediate results from the alkene insertion into the Ir–alkenyl bond of intermediate **II** with a 1,2-regioselectivity, followed by β -H elimination. It should be noted that this 1,2 insertion is disfavored with respect to 2,1 insertion leading to the main hydroalkenylation product (Scheme 4). In addition, the formation of the hydroalkenylation products **10** requires the tautomerization of the 3-*R*-4*H*-quinolizine derivatives to the 3-*R*-6*H*-quinolizine ones (Scheme 7). This could be promoted by the presence of free acetylacetonate in the reaction media which, in principle, has the ability to deprotonate the $>CH_2$ moiety at position 4 of the 4*H*-quinolizine skeleton (**III**), rendering acetylacetonate which on its turn protonates at a different position as a consequence of a charge movement affording a new quinolizine tautomer (**IV–VI**).



Scheme 6. Proposed mechanism for the formation of **10** in the hydroalkenylation of phenylacetylene with 2-vinylpyridine catalyzed by **6**.



Scheme 7. Proposed sequence for the formation of **10a** along with the relative Gibbs free energy of the intermediates (italics, kcal mol⁻¹) under metal-free conditions.

Finally, the retro-electrocyclization of **IV** would afford the unusual (*Z*)-2-(buta-1,3-dien-1-yl)-5*R*-pyridine (**VII**; Scheme 7). Remarkably this mechanism nicely explains the outcome of the reaction between 2-vinylpyridine and [D]phenylacetylene. In particular, the high degree of deuteration of one of the >CH₂ protons in the observed 4*H*-quinolizine intermediate and the position C-2 of the pyridinyl moiety of **10a** give support to the proposed mechanism. The acetylacetonate anion should be also responsible for the H/D exchange reaction of phenylacetylene which, in turn, accounts for up to 30% incorporation of H at the *E*-olefin moiety of the butadienyl fragment in **9a** (Scheme 5).

It is noteworthy that the 4*H*-quinolizine intermediate (**III**) was only observed at trace levels in the hydroalkenylation of unlabeled phenylacetylene, which suggests that the tautomerization/retro-electrocyclization reaction of the 4*H*-[D]quinolizine is slower due to the presence of C–D methylene bonds. Finally, we have studied the reaction of 3-phenyl-4*H*-quinolizine (**III**) with acac⁻ and Hacac observing in both cases the formation of **10a**. Nevertheless, extensive decomposition was also observed which indicates that the Ir(acac)(IPr) metal fragment might be active in the tautomerization process, as well.

Looking for further support for the proposed isomerization sequence given in Scheme 7, the relative energies of the intermediates I–VIII have been calculated. It is noteworthy that all the intermediates are accessible under the experimental conditions and that the most stable species is **VIII** (*G*_{rel} =

+3.7 kcal mol⁻¹), that is (*Z*)-2-(buta-1,3-dien-1-yl)-5-phenylpyridine (**10a**), nicely agreeing with the observed outcome of the reaction. In addition, 3-phenyl-4*H*-quinolizine (**III**) is the second most stable species (*G*_{rel} = +2.6 kcal mol⁻¹), which nicely matches the fact that it has been observed in trace amounts in the course of the catalytic reaction.

Conclusion

The cyclometalated complex IrH(κ²O, O'-acac)(κ²N, C-(C₇H₆N)(IPr) (**6**) has been revealed as an efficient catalyst for the hydroalkenylation of terminal alkynes with 2-vinylpyridine to selectively afford butadienylpyridine derivatives. A range of aromatic and aliphatic terminal alkynes, as well as enynes were subjected to hydroalkenylation to give 2-((1*Z*,3*E*)-4*R*-buta-1,3-dien-1-yl)pyridine derivatives as major reaction products, and the (*Z*)-2-(buta-1,3-dien-1-yl)-5*R*-pyridine isomers. As a general trend, aromatic alkynes react faster than aliphatic ones, with the exception of aromatic alkynes containing electron-withdrawing substituents. In addition, no isomerization of the butadiene fragment was observed under catalytic conditions. The main reaction products formally result from the *syn* addition of 2-vinylpyridine to the terminal alkyne whereas the unexpected butadienylpyridine derivative arises from the undetected 2-((1*Z*,3*gem*)-3*R*-buta-1,3-dien-1-yl)pyridine hydroalkenylation intermediates. These elusive compounds should undergo a facile thermal 6π-electrocyclization to afford the bicyclic 4*H*-quinolizine derivative that, under the reaction conditions, tautomerizes to 6*H*-quinolizine to afford the (*Z*)-2-(buta-1,3-dien-1-yl)-5*R*-pyridine by a retro-electrocyclization reaction. Consistent with this proposal, deuterium labeling studies using [D]phenylacetylene have shown that the tautomerization/retro-electrocyclization of the 4*H*-[D]quinolizine derivative is slower than that of the unlabeled derivative.

Reactivity studies and related precedents in phosphine chemistry have allowed us to propose a mechanism that proceeds via iridium(III) intermediates. Sequential alkyne and 2-vinylpyridine activation in IrH(κ²O, O'-acac)(κ²N, C-C₇H₆N)(IPr) results in the formation of a cationic η²-alkene species with two κ²N, C-alkenyl-pyridine ligands as the key intermediate. Subsequent alkene insertion into the coplanar iridium–alkenyl bond results in an unsaturated intermediate featuring a seven-membered metallacycle from which β-hydride elimination leads to the formation of butadienylpyridine products. Interestingly, the regioselectivity of the alkene insertion, which is proposed to be the rate-determining step, determines the formation of the 1*Z*,3*E*- or 1*Z*,3*gem*-butadienyl derivatives. The observation of terminal alkenes in trace amounts in most of the catalytic runs and the determination of an inverse kinetic isotope effect give support to the proposed mechanism.

The presence of the IPr carbene and BHetA ligands in the catalysts are likely decisive for the catalytic outcome. First, the steric influence of the IPr ligand directs the regioselectivity of the alkene insertion reaction leading to the major formation of the lineal 2-(4*R*-butadienyl)pyridine derivatives. On the other hand, the lability of the BHetA ligand allows both the

generation of the vacant sites required for the coupling events and the stabilization of reaction intermediates.

Experimental Section

Detailed synthetic procedures and characterization of organo-metallic complexes and NMR data for organic compounds are available in the Supporting Information.

Preparation of IrH(κ^2 O,O'-acac)(κ^2 N,C-C₇H₆N)(IPr) (6): A solution of **3** (100 mg, 0.130 mmol) in toluene (5 mL) was treated with 2-vinylpyridine (21.0 μ L, 0.200 mmol) and stirred for 15 h at 60 °C. After filtration through Celite, the solution was brought to dryness in vacuo. Addition of cold hexane induced the precipitation of a pale orange solid, which was washed with hexane (3 x 4 mL) and dried in vacuo. Yield: 80.0 mg (78%). HRMS (ESI⁺, CH₃CN, *m/z*): Calcd for C₃₉H₅₁N₃O₂Ir (M + H⁺) 786.3605; found: 786.3592. ¹H NMR (400 MHz, C₆D₆, 298 K): δ 10.04 (d, *J*_{H-H} = 8.0, 1H, Ir-CH=CH), 8.11 (d, *J*_{H-H} = 5.4, 1H, H_{6-py}), 7.25 (d, *J*_{H-H} = 6.6, 4H, H_{m-IPr}), 7.19 (d, *J*_{H-H} = 8.0, 1H, Ir-CH=CH), 7.14 (t, *J*_{H-H} = 6.6, 2H, H_{p-IPr}), 6.8–6.7 (2H, H_{3,4-py}), 6.68 (s, 2H, =CHN), 6.30 (dd, *J*_{H-H} = 8.5, 5.4, 1H, H_{5-py}), 4.92 (s, 1H, CH_{acac}), 3.61 and 3.21 (both sept, *J*_{H-H} = 6.4, 4H, CHMe_{IPr}), 1.98 and 1.01 (both s, 6H, Me_{acac}), 1.70, 1.48, 1.30, and 1.26 (all d, *J*_{H-H} = 6.4, 24H, CHMe_{IPr}), –26.70 (s, 1H, Ir-H). ¹³C{¹H}-APT NMR (100.4 MHz, C₆D₆, 298 K): δ 184.3 and 182.1 (C_{q-acac}), 169.1 (C_{2-py}), 166.6 (Ir-CH=CH), 162.0 (Ir-C_{IPr}), 147.5 (C_{6-py}), 146.8 and 145.4 (C_{q-IPr}), 138.8 (C_{qN}), 135.7 (C_{4-py}), 128.9, 123.6, and 123.3 (CH_{ph}), 128.7 (Ir-CH=CH), 123.4 (=CHN), 117.5 (C_{3-py}), 115.0 (C_{5-py}), 99.9 (CH_{acac}), 28.5 and 28.5 (CHMe_{IPr}), 28.3 and 27.5 (Me_{acac}), 25.9, 25.5, 23.0, and 23.0 (CHMe_{IPr}).

Standard catalytic reactions: An NMR tube was charged under argon with the catalyst (0.01 mmol), C₆D₆ (0.5 mL), 2-vinylpyridine (0.15 mmol), the corresponding terminal alkyne (0.15 mmol) and mesitylene (0.015 mmol) as internal standard. Then, the NMR tube was sealed, heated at 90 °C and monitored by ¹H NMR spectroscopy. Conversion and selectivities were determined by integration of the corresponding resonances of 2-vinylpyridine and those of the reaction products.

The catalytic solutions were transferred to a small flask and the solvent removed under vacuum. The dark residue was purified by silica gel column chromatography eluting with hexane/diethyl ether (90:10) to afford the 2-{buta-1,3-dien-1-yl}-pyridine derivatives (**9** and **10**) as colorless oils.

Crystal structure determination: Deposition Numbers 2073904 (for **3**), 2073894 (for **5**), 2073899 (for **6**), and 2073901 (for **7**) contains the supplementary crystallographic data for this paper. These data are provided free of charge by the joint Cambridge Crystallographic Data Centre and Fachinformationszentrum Karlsruhe Access Structures service www.ccdc.cam.ac.uk/structures.

Acknowledgements

Financial support from the Spanish Ministerio de Ciencia e Innovación (MICINN/FEDER) under Project PID2019-103965GB-I00, and the Departamento de Ciencia, Universidad y Sociedad del Conocimiento del Gobierno de Aragón (group E42_20R) is gratefully acknowledged. I.G. thanks the Humboldt Foundation for a research fellowship.

Conflict of Interest

The authors declare no conflict of interest.

Keywords: C–H activation · C–C coupling · catalysis · hydroalkenylation · iridium · N-heterocyclic carbenes

- [1] a) F. Kakiuchi, S. Murai, *Acc. Chem. Res.* **2002**, *35*, 826–834; b) J. Wencel-Delord, T. Droge, F. Liu, F. Glorius, *Chem. Soc. Rev.* **2011**, *40*, 4740–4761; c) J.-P. Wang, L. Gan, Y. Liu, *Org. Biomol. Chem.* **2017**, *15*, 9031–9043; d) C.-S. Wang, P. H. Dixneuf, J.-F. Soulé, *Chem. Rev.* **2018**, *118*, 7532–7585; e) P. Gandeepan, N. Kaplaneris, S. Santoro, L. Vaccaro, L. Ackermann, *ACS Sustainable Chem. Eng.* **2019**, *7*, 8023–8040.
- [2] a) S. Roscales, I. G. Salado, A. G. Csáky, *Synlett* **2011**, *15*, 2234–2236; b) X. Zhou, A. Chen, W. Du, Y. Wang, Y. Peng, H. Huang, *Org. Lett.* **2019**, *21*, 9114–9118; c) J. Han, J. Kim, J. Lee, Y. Kim, S. Y. Lee, *J. Org. Chem.* **2020**, *85*, 15476–15487; d) K. P. S. Cheung, D. Kurandina, T. Yata, V. Gevorgyan, *J. Am. Chem. Soc.* **2020**, *142*, 9932–9937; e) J.-J. Tian, Z.-Y. Yang, X.-S. Liang, N. Liu, C.-Y. Hu, X.-S. Tu, X. Li, X.-C. Wang, *Angew. Chem. Int. Ed.* **2020**, *59*, 18452–18456; *Angew. Chem.* **2020**, *132*, 18610–18614.
- [3] a) J. L. Gage, H. A. Kirst, D. O'Neil, B. A. David, C. K. Smith II, S. A. Naylor, *Bioorg. Med. Chem.* **2003**, *11*, 4083–4091; b) U. Groenohagen, M. Maczka, J. S. Dickschat, *Beilstein J. Org. Chem.* **2014**, *10*, 1421–1432.
- [4] a) D.-J. Dong, H.-H. Li, S.-K. Tian, *J. Am. Chem. Soc.* **2010**, *132*, 5018–5020; b) Q.-Q. Li, Z. Shah, J.-P. Qu, Y.-B. Kang, *J. Org. Chem.* **2018**, *86*, 296–302.
- [5] a) M. Lemhadri, A. Battace, F. Berthiol, T. Zair, H. Doucet, M. Santelli, *Synthesis* **2008**, *7*, 1142–1152; b) V. T. Nguyen, H. T. Dang, H. H. Pham, V. D. Nguyen, C. Flores-Hansen, H. D. Arman, O. V. Larionov, *J. Am. Chem. Soc.* **2018**, *140*, 8434–8438.
- [6] a) L. R. Eastman Jr., B. M. Zarnegar, J. M. Butler, D. G. Whitten, *J. Am. Chem. Soc.* **1974**, *96*, 2281–2283; b) G. Bartocci, G. Galiazzo, L. Latterini, E. Marri, U. Mazzucato, A. Spalletti, *Phys. Chem. Chem. Phys.* **2002**, *4*, 2911–2916.
- [7] a) V. Boekelheide, W. G. Gall, *J. Am. Chem. Soc.* **1954**, *76*, 1832–1836; b) T. Miyadera, Y. Kishida, *Tetrahedron* **1969**, *25*, 397–413; c) G. M. Sanders, M. van Dijk, H. C. van der Plas, M. Konijn, C. H. Stam, *J. Heterocycl. Chem.* **1983**, *20*, 407–413.
- [8] a) C. S. Yi, D. W. Lee, Y. Chen, *Organometallics* **1999**, *18*, 2043–2405; b) S. J. Blanksby, G. B. Ellison, *Acc. Chem. Res.* **2003**, *36*, 255–263.
- [9] a) S. Oi, K. Sakai, Y. Inoue, *Org. Lett.* **2005**, *7*, 4009–4011; b) Y. Huang, W.-J. Pana, Z.-X. Wang, *Org. Chem. Front.* **2019**, *6*, 2284–2290.
- [10] a) Y. Nakao, K. S. Kanyiva, T. Hiya, *J. Am. Chem. Soc.* **2008**, *130*, 2448–2449; b) Y. Kuninobu, Y. Fujii, T. Matsuki, Y. Nishina, K. Takai, *Org. Lett.* **2009**, *11*, 2711–2714; c) R. Azpiroz, A. Di Giuseppe, R. Castarlenas, J. J. Pérez-Torrente, L. A. Oro, *Chem. Eur. J.* **2013**, *19*, 3812–3816; d) R. Azpiroz, A. Di Giuseppe, V. Passarelli, J. J. Pérez-Torrente, L. A. Oro, R. Castarlenas, *Organometallics* **2018**, *37*, 1695–1707.
- [11] a) W. Hermann, *Angew. Chem. Int. Ed.* **2002**, *41*, 1290–1309; *Angew. Chem.* **2002**, *114*, 1342–1363; b) S. Díez-González, N. Marion, S. P. Nolan, *Chem. Rev.* **2009**, *109*, 3612–3676; c) D. J. Müller, C. Schleppehorst, F. Glorius, *Chem. Soc. Rev.* **2017**, *46*, 4845–4854; d) E. Peris, *Chem. Rev.* **2018**, *118*, 9988–10031; e) Q. Zhao, G. Meng, S. P. Nolan, M. Szostak, *Chem. Rev.* **2020**, *120*, 1981–2048.
- [12] a) G. Sipos, R. Dorta, *Coord. Chem. Rev.* **2018**, *375*, 13–78; b) M. Iglesias, L. A. Oro, *Chem. Soc. Rev.* **2018**, *47*, 2772–2708.
- [13] a) M. C. Perry, X. Cui, M. T. Powell, D.-R. Hou, J. H. Reibenspies, K. Burgess, *J. Am. Chem. Soc.* **2003**, *125*, 113–123; b) A. Schumacher, M. Bernasconi, A. Pfaltz, *Angew. Chem. Int. Ed.* **2013**, *52*, 7422–7425; *Angew. Chem.* **2013**, *125*, 7570–7573; c) X. Quan, S. Kerdphon, B. B. C. Peters, J. Rujirawanich, S. Krajangsri, J. Jongcharoenkamol, P. G. Andersson, *Chem. Eur. J.* **2020**, *26*, 13311–13316.
- [14] a) A. Zanardi, E. Peris, J. A. Mata, *New J. Chem.* **2008**, *32*, 120–126; b) M. Iglesias, P. J. Sanz Miguel, V. Polo, F. J. Fernández-Alvarez, Jesús J. Pérez-Torrente, Luis A. Oro, *Chem. Eur. J.* **2013**, *19*, 17759–17566; c) A. I. Ojeda-Amador, J. Munarriz, P. Alamán-Valtierra, V. Polo, R. Puerta-Oteo, M. V. Jiménez, F. J. Fernández-Alvarez, J. J. Pérez-Torrente, *ChemCatChem* **2019**, *11*, 5524–5535.
- [15] a) R. Corberán, M. Sanaú, E. Peris, *J. Am. Chem. Soc.* **2006**, *128*, 3974–3979; b) W. J. Kerr, M. Reid, T. Tuttle, *Angew. Chem. Int. Ed.* **2017**, *56*, 7808–7812; *Angew. Chem.* **2017**, *129*, 7916–7920; c) D. S. Timofeeva, D. M. Lindsay, W. J. Kerr, D. J. Nelson, *Catal. Sci. Technol.* **2020**, *10*, 7249–7255.

- [16] a) A. Prades, R. Corberán, M. Poyatos, E. Peris, *Chem. Eur. J.* **2008**, *14*, 11474–11479; b) M. V. Jiménez, J. Fernández-Tornos, F. J. Modrego, J. J. Pérez-Torrente, L. A. Oro, *Chem. Eur. J.* **2015**, *21*, 17877–17889; c) J. Wu, L. Shen, Z.-N. Chen, Q. Zheng, X. Xu, T. Tu, *Angew. Chem. Int. Ed.* **2020**, *59*, 10421–10425; *Angew. Chem.* **2020**, *132*, 10507–10511.
- [17] a) N. Imlinger, M. Mayr, D. Wang, K. Wurst, M. R. Buchmeiser, *Adv. Synth. Catal.* **2004**, *346*, 1836–1843; b) A. Zanardi, J. A. Mata, E. Peris *J. Am. Chem. Soc.* **2009**, *131*, 14531–14537; c) L. Rubio-Pérez, M. Iglesias, J. Munárriz, V. Polo, P. J. Sanz Miguel, J. J. Pérez-Torrente, L. A. Oro, *Chem. Commun.* **2015**, *51*, 9860–9863; d) C. Yang, F. Mehmood, T. L. Lam, S. L.-F. Chan, Y. Wu, C.-S. Yeung, X. Guan, K. Li, C. Y.-S. Chung, C.-Y. Zhou, T. Zou, C.-M. Che, *Chem. Sci.* **2016**, *7*, 3123–3136; e) C.-C. Bao, D.-S. Zheng, X. Zhang, S.-L. You, *Organometallics* **2018**, *37*, 4763–4772.
- [18] a) B. DeBoef, S. J. Pastine, D. Sames, *J. Am. Chem. Soc.* **2004**, *126*, 6556–6557; b) T. Iwai, T. Fujihara, J. Terao, Y. Tsuji, *J. Am. Chem. Soc.* **2012**, *134*, 1268–1274; c) C. D. Forsyth, W. J. Kerr, L. C. Paterson, *Synlett* **2013**, *24*, 587–590.
- [19] a) N. M. Scott, V. Pons, E. D. Stevens, D. M. Heinekey, S. P. Nolan, *Angew. Chem. Int. Ed.* **2005**, *44*, 2512–2515; *Angew. Chem.* **2005**, *117*, 2568–2571; b) C. Y. Tang, W. Smith, D. Vidovic, A. L. Thompson, A. B. Chaplin, S. Aldridge, *Organometallics* **2009**, *28*, 3059–3066; c) N. Phillips, C. Y. Tang, R. Tirfoin, M. J. Kelly, A. L. Thompson, M. J. Gutmann, S. Aldridge, *Dalton Trans.* **2014**, *43*, 12288–12298.
- [20] a) A. H. Janowicz, R. G. Bergman, *J. Am. Chem. Soc.* **1983**, *105*, 3929–3939; b) Y. Alvarado, O. Boutry, E. Gutierrez, A. Monge, M. C. Nicasio, M. L. Poveda, P. J. Pérez, C. Ruiz, C. Bianchini, E. Carmona, *Chem. Eur. J.* **1997**, *3*, 860–873; c) J. Oxgaard, G. Bhalla, R. A. Periana, W. A. Goddard III, *Organometallics* **2006**, *25*, 1618–1625.
- [21] a) Ł. Woźniak, J.-F. Tan, Q.-H. Nguyen, A. Madron du Vigné, V. Smal, Y.-X. Cao, N. Cramer, *Chem. Rev.* **2020**, *120*, 105160–10543; b) D. F. Fernández, J. L. Mascareñas, F. López, *Chem. Soc. Rev.* **2020**, *49*, 7378–7405.
- [22] D. Balcells, E. Clot, O. Eisenstein, *Chem. Rev.* **2010**, *110*, 749–823.
- [23] J. Navarro, E. Sola, M. Martín, I. T. Dobrinovitch, F. J. Lahoz, L. A. Oro, *Organometallics* **2004**, *23*, 1908–1917.
- [24] a) Y. Sun, K. Meng, J. Zhang, M. Jin, N. Huang, G. Zhong, *Org. Lett.* **2019**, *21*, 4868–4872; b) Q.-L. Yang, Y.-K. Xing, X.-Y. Wang, H.-X. Ma, X.-J. Weng, X. Yang, H.-M. Guo, T.-S. Mei, *J. Am. Chem. Soc.* **2019**, *141*, 18970–18976; c) Y. Huang, L. Xu, F. Yu, W. Shen, X. Lu, L. Ding, L. Zhong, G. Zhong, J. Zhang, *J. Org. Chem.* **2020**, *85*, 7225–7237; d) X. Sun, W. Zhao, B.-J. Li, *Chem. Commun.* **2020**, *56*, 1298–1301.
- [25] a) T. Shibata, T. Baba, H. Takano, K. S. Kanyiva, *Adv. Synth. Catal.* **2017**, *359*, 1849–1853; b) D. F. Fernández, C. A. B. Rodrigues, M. Cavelo, M. Gullías, J. L. Mascareñas, F. López, *ACS Catal.* **2018**, *8*, 7397–7402.
- [26] M. Galiana-Cameo, M. Borraz, Y. Zelenkova, V. Passarelli, F. J. Lahoz, J. J. Pérez-Torrente, L. A. Oro, A. Di Giuseppe, R. Castarlenas, *Chem. Eur. J.* **2020**, *26*, 9598–9608.
- [27] M. A. Bennett, D. J. Patmore, *Inorg. Chem.* **1971**, *10*, 2387–2395.
- [28] R. Azpiroz, L. Rubio-Pérez, A. Di Giuseppe, V. Passarelli, F. J. Lahoz, R. Castarlenas, J. J. Pérez-Torrente, L. A. Oro, *ACS Catal.* **2014**, *4*, 4244–4253.
- [29] L. Palacios, A. Di Giuseppe, R. Castarlenas, F. J. Lahoz, J. J. Pérez-Torrente, L. A. Oro, *Dalton Trans.* **2015**, *44*, 5777–5789.
- [30] M. V. Jiménez, J. Fernández-Tornos, J. J. Pérez-Torrente, F. J. Modrego, P. García-Orduña, L. A. Oro, *Organometallics* **2015**, *34*, 926–940; b) R. Puerta-Oteo, M. V. Jiménez, F. J. Lahoz, F. J. Modrego, V. Passarelli, J. J. Pérez-Torrente, *Inorg. Chem.* **2018**, *57*, 5526–5543.
- [31] L. Palacios, A. Di Giuseppe, A. Opalinska, R. Castarlenas, J. J. Pérez-Torrente, F. J. Lahoz, L. A. Oro, *Organometallics* **2013**, *32*, 9, 2768–2774.
- [32] R. N. Perutz, S. Sabo-Etienne, *Angew. Chem. Int. Ed.* **2007**, *46*, 2578–2592; *Angew. Chem.* **2007**, *119*, 2630–2645.
- [33] M. Gómez-Gállego, M. A. Sierra, *Chem. Rev.* **2011**, *111*, 4857–4963.
- [34] Y. Zhang, M. K. Karunananda, H.-C. Yu, K. J. Clark, W. Williams, N. P. Mankad, D. H. Ess, *ACS Catal.* **2019**, *9*, 2657–2663.
- [35] D. G. Churchill, K. E. Janak, J. S. Wittenberg, G. Parkin, *J. Am. Chem. Soc.* **2003**, *125*, 1403–1420.

Manuscript received: April 20, 2021

Accepted manuscript online: May 17, 2021

Version of record online: June 21, 2021